EUROPEAN ORGANIZATION FOR NUCLEAR RESEARCH

PH I/COM-70/63
8 December, 1970

PHYSICS I

ELECTRONICS EXPERIMENTS COMMITTEE

PROPOSAL FOR A SYSTEMATIC STUDY OF THE STRANGENESS ZERO, CHARGED BOSON SPECTRUM USING THE OMEGA AND A PROTON TIME OF FLIGHT TRIGGER

by

N. Armenise, V. Picciarelli, A. Romano, A. Silvestri
University of Bari - I.N.F.N. Bari

U. Idschock, B. Nellen, K. Müller - University of Bonn

H.W. Atherton, J. Eades, B. French, B. Ghidini[+], A. Grant, L. Mandelli[++], J. Moebes, F. Navach, CERN

G. Bellini, A. Cantore, M. di Corato, M.P. Manfredi, G. Vegni
University of Milan - I.N.F.N. Milan (*)

TO BE SUBMITTED TO
THE E.E.C.

CERN /D.Ph.II/PHYS - 70-66
1.12.1970

PROPOSAL FOR A SYSTEMATIC STUDY OF THE STRANGENESS ZERO, CHARGED BOSON SPECTRUM USING THE OMEGA AND A PROTON TIME OF FLIGHT TRIGGER.

N. Armenise, V. Picciarelli, A. Romano, A. Silvestri
University of Bari - I.N.F.N. Bari

U. Idschock, B. Nellen K. Müller - University of Bonn

H.W. Atherton, J. Eades, B. French, B. Ghidini[+], A. Grant, L. Mandelli[++], J. Moebes, F. Navach, CERN

G. Bellini, A. Cantore, M. di Corato, M.P. Manfredi, G. Vegni
University of Milan - I.N.F.N. Milan (*)

1. INTRODUCTION

The systematic study of the boson mass spectrum by the CERN missing mass experiments [1] has revealed an apparent regularity in the $(\text{mass})^2$ for those resonances produced with cross-sections above a certain value. Many questions are raised by the M.M.S. results. For example one may ask the following :

a) Does the fact that the resonances with relatively high cross-sections show a regularity mean that we are in some way seeing the "principal series" of the meson system as was the case for the hydrogen atom? If so, then it is clearly of interest to study this series in more detail. In particular does the series have the expected $(\text{mass})^2$ versus J^P relationship indicated by Regge theory? This relation

---

* R.A. Donald, D.N. Edwards and J. Fry of the University of Liverpool are also seriously considering joining this proposal.

\+ On leave of absence from the University of Bari

++ On leave of absence from the University of Milan

CERN/D.Ph.II/ PHYS 70-66
1.12.1970

seems valid for the ρ^- and A_2^- mesons but the situation in and above the so called R region(at a mass around 1.7 GeV/c^2) is, as yet, unclear. The R-region, which is below the $N\bar{N}$ threshold, is only accessible by production experiments. However, even above the $N\bar{N}$ threshold it will be important to establish the properties of the resonances in the series produced via production as they may be completely different to the resonancesformed in $N\bar{N}$ formation experiments. As Astier[2] has pointed out, the πp and $N\bar{N}$ experiments are two different fishing nets and do not necessarily catch the same fish. Comparison of the fish caught will be interesting.

b) Does the R-region have really a fine structure as suggested by the M.M.S. experiments and if so can it be understood in terms of the spin-orbit splitting of the quark model[3]? For this it will be necessary to establish the J^P and I^G of each resonance.

c) Why are the widths found by the M.M.S. experiments apparently narrower than those seen in the hydrogen bubble chamber experiments ?

d) Is there a dependence of the production, position and width of a resonance on the momentum transfer at which it is produced ?

e) What is the mechanism of decay of the higher mass resonances ? Do they prefer to decay into two roughly equal mass objects (fission)[4] or do they prefer to decay via single pion emission (cascade decay) ? Do the decay products belong to the same series or do they lie on another trajectory ?

f) Are there other meson series produced with lower cross-sections, than the principal series, having different t dependence and/or different variation with the centre of mass energy ?

CERN/D.Ph.II/PHYS 70-66
1.12.1970

For answering these questions we believe the following properties which the OMEGA has, should result in our having a good chance of improving considerably the understanding in this field.

i) almost 4π solid angle for charged particle detection, a fact which is important for unbiased spin-parity analyses of boson resonances with multiparticle decays;

ii) accurate momentum and angle measurement of all secondary charged particles à la bubble chamber, necessary for isolating individual reaction channels, determining J^P, G parity and branching ratios, and increasing the signal to background ratio of resonances;

iii) the possibility of triggering on the boson mass region of interest;

iv) the possibility of obtaining a factor of ~ 100 in number of events over present bubble chamber data in the given boson mass region studied;

v) a missing mass error in the region of $\pm$ 10 to $\pm$ 15 MeV, similar to that of the CERN M.M.S. experiment;

vi) an error on the effective mass of the charged particle secondaries of $\pm$ 5 MeV.

One region which seems, to us, of interest at the present time is the so called R-region (mass at 1.7 GeV/c^2) and it is this region we would like to study first. (However, it seems reasonable that, in the future, a systematic study of the whole region explored by the M.M.S. experiment will be important).

Several recent experiments either with the bubble chamber or the counter missing mass techniques have shown the existence of several boson resonances in the mass region near 1.7 GeV/c^2 [2]. Missing mass experiments have shown the existence of four peaks in the $I \geq 1$ mass spectrum (R_1, R_2, R_3, R_4) with unknown quantum numbers

and decay modes. The widths are all less than 40 MeV. On the other hand the bubble chamber technique has shown the existence of at least two different states with $\Gamma > 40$ MeV : a) $I^G = 1^+$ decaying into two and/or four pions and b) $I^G = 1^-$ decaying into a 3π system. How these states are connected with those found by the missing mass spectrometer is, as yet, an open question.

This proposal involves collecting 10^6 events in the R-region and would mean approximately 10 days running time at the P.S.

2. METHOD AND TRIGGERING

We propose to study in the OMEGA apparatus the reaction

$$\pi^- p \rightarrow p\, X^- \qquad (1)$$

The events are triggered using a time of flight proton trigger arranged to select a missing mass to the proton (M_{X^-}) in the region 1.5 - 2.0 GeV/c^2.

For this experiment we intend to make no selection on the other charged secondaries in order to first reproduce the results of the M.M.S. experiment[1] and then, by measuring all charged secondary and using kinematic fitting, to analyse separately the different final states. The most abundant of these are :

$$\pi^- p \rightarrow p\, X^- \qquad (2)$$

$$\left.\begin{array}{l} \hookrightarrow \pi^-\pi^0 \\ \pi^- X^0 \\ \pi^+\pi^-\pi^- \\ \pi^+\pi^-\pi^-\pi^0 \\ \pi^+\pi^-\pi^- X^0 \\ \pi^+\pi^+\pi^-\pi^-\pi^- \end{array}\right\}$$

Smaller samples of the following interesting final states will also be obtained :

CERN/D.Ph.II/PHYS 70-66
1.12.1970

$$\pi^- p \rightarrow p X^- \longrightarrow \begin{cases} K^0 K^- \\ K^0 K^- \pi^0 \\ K^0 K^0 \pi^- \\ K^0 K^0 \pi^- \pi^0 \\ K^+ K^- \pi^- \\ K^0 K^\mp \pi^\pm \pi^- \end{cases} \qquad (3)$$

If, after analysis, some of these latter channels, e.g. K^0K^-, prove interesting, a separate run to select them could be envisaged using, for example, proportional chambers. For the two body reactions (1) the momentum and the production angle of the recoil proton in the laboratory are kinematically related for a given value of M_X-. Figs. 1a and 1b show this dependence for incident momenta of 12 and 8 GeV/c respectively Fig.2a shows the trajectories of protons corresponding to a mass of 1.7 GeV/c^2 and an incident momentum of 12 GeV/c which satisfy the requirement that they leave the spark chamber system at the side opposite to their emission direction, so that they may be well measured.

For a given mass (M_X-) the locus of protons, after a given time of flight, is approximately a straight line in a plane perpendicular to the OMEGA magnetic field. The loci for various masses at the same instant of time are slightly different. Fig. 2 shows, for M_X = 1.7 GeV/c^2, the loci at 15, 20, 25 and 30 ns along with the loci at 25ns for M_X- in the range 1.4 - 2.0 GeV/c^2. The principle of the trigger consists in placing a scintillation counter at the locus of a mass in the middle of the wanted mass region and selecting a region of mass around this value by using a suitable time gate (see App. 1 for details). The correlation between the time of arrival of protons at the counter (placed at the locus of 25 ns for M_X = 1.7 GeV/c^2) and the corresponding missing mass M_X, is shown in fig. 3 where the plotted events are obtained by a Montecarlo method. It can be seen from fig. 3 that it is possible to change the selected

mass region by simply varying the time interval, e.g. for the region 1.5 - 1.9 GeV an interval 22 - 26 ns is necessary. Fig. 4 shows the distribution of arrival times of pions and protons at the locus. It can be seen that by choosing a time of flight $\geq$15 ns only triggers on protons will occur.

3. ACCEPTANCE AND TRIGGERING RATES

The acceptance of the proposed trigger is a function of M_X and $-t_{p/p}$ (the square of the four momentum transfer to the proton). Fig. 5a shows the triggering acceptance as a function of M_X integrated over $-t_{p/p}$ The upper curve shows the solid angle effect, what we can call the "geometrical acceptance"; the lower one shows the effect of a time gate (22 - 26 ns). It is important to note that in the interesting region the acceptance is only the geometrical one. Fig. 5b shows the triggering acceptance as a function of $-t_{p/p}$ integrated over the mass interval 1.5 - 2.0 GeV^2 This acceptance is due to the solid angle effect only.

The fact that the selected protons have momenta in the range (0.3 - 0.7) GeV/c means that $t_{p/p}$ covers the region (0.09 - 0.44) GeV^2. Comparing this with the missing mass spectrometer, which explored a t interval of (0.23 - 0.28) GeV^2, we see that the t region in this proposal is a factor 7 wider. Moreover, since the momentum of the recoil proton is measured accurately the mass resolution changes little with t even when the kinematic configuration is not that of the Jacobian peak. Since the t range studied here includes a large part of the reaction cross-section studied with bubble chambers, it should be possible to explore the wanted mass region as a function of t to see if there is a t dependence of the resonance production, which might go part way to explaining the difference in the resonance widths as found by the missing mass and bubble chamber techniques.

CERN/D.Ph.II/PHYS 70-66
1.12.1970

Fig. 6 shows the plot $-t_{p/p}$ vs M_X for a physical sample of four pronged events at 11.2 GeV/c with the projections on the two axes. The shaded areas show the triggered region. To obtain mean triggering efficiencies and triggering rates for reactions (2) we have used events from a $\pi^- p$ H.B.C. experiment at 11.2 GeV/c,* traced them in the OMEGA, and simulated the trigger.

Tables 1a and b give the percentages of events of the more abundant reactions triggering the apparatus along with the total triggering cross-sections and the numbers of events expected for 10^6 good triggers.

For example, in the reaction $\pi^- p \rightarrow p\pi^+\pi^-\pi^-$ at 11.2 GeV/c we should obtain about 200'000 events which may be compared to about 1000 events in the same mass region from a typical bubble chamber experiment at the present time. Assuming a beam intensity of 3.10^5 π's/burst and a 20 cm long H_2 target, the triggering rate is of the order of 12 events/burst. With an assumed mean rate of picture taking of 6 per burst and a 50 % running efficiency, 120,000 events/day could be achieved (or $\sim 10^6$ in 8 days). Besides reactions (2) there are smaller, but not uninteresting samples of reactions (3). Typical cross-sections being 50 ns and typical acceptances 0.5 %, we obtain for each of them ~5000 events. In order to calculate the number of events we can expect in a resonance above the background, we have used the cross-sections for the peaks found by the M.M.S. (R1, R2, R3), and for some of the resonances found in H.B.C. experiments involving 100,000 - 200,000 pictures. in the 2m H.B.C. . Applying the acceptance curve shown in fig. 5a we arrive at the results shown in table 2. Factors of 100 increase over present day samples seem reasonable to expect.

4. EVALUATION OF ERRORS

As explained in detail in appendix 2, events have been traced in the OMEGA, and from the calculated errors on $\frac{1}{\rho}, \lambda, \varphi$ for

* We wish to thank the G.H.M.S. collaboration and the ABC collaboration who kindly loaned us their data on 11.2 GeV/c $\pi^- p$ and 8 GeV/c $\pi^+ p$ respectively

CERN/D.Ph.II/PHYS 70.66
1.12.1970

each track, errors on the most interesting quantities have been derived.

Figs. 7a and 7b show the scatter plots of the error on M_X (σ_{M_X}) vs $-tp/p$ at incident momenta of 12 and 8 GeV/c for the following error contributions :

a) total error σ_{M_X},
b) error σ_{M_X} due to the setting error on individual sparks,
c) errors σ_{M_X} due to scattering in the chambers,
d) errors σ_{M_X} due to scattering in Mylar around the target (.03 cm),
e) errors σ_{M_X} due to scattering in the hydrogen of the target,
f) errors σ_{M_X} due to errors on the beam track

$$\left(\frac{\Delta P}{P} = 0.3\ ^{o}/_{o},\ \Delta\varphi = \Delta\lambda = 1\ \text{mrad}\right)$$

For these and similar plots the errors at three values for the four momentum transfer were derived and are given in tables 3a and 3b. It is interesting to note that in the region $-t_{p/p} \simeq 0.25\ (\text{GeV/c}^2)^2$ the error on M_X is of the same order ($\pm$ 13 MeV at 12 GeV/c) or better ($\pm$ 9.5 MeV at 8 GeV/c) than that quoted in the M.M.S. experiment for the R region ($\pm$ 15 MeV)[1]. Figs. 8a and 8b show the distribution of the errors on the 3π and 2π masses at 8 GeV/c and 12 GeV/c respectively. The mean values, of $\sigma_{2\pi} = \pm$ 5.5 MeV, $\sigma_{3\pi} = \pm$ 8.5 MeV at 12 GeV/c and $\sigma_{2\pi} = \pm$ 5.2 MeV, $\sigma_{3\pi} = \pm$ 7.5 MeV at 8 GeV/c, are also listed in tables 3a and 3b. This means that for the reaction $\pi^- p \rightarrow p\pi^-\pi^-\pi^+$ the resolution on M_X is improved to $\sigma_{M_X} = \pm$ 8.5 MeV. The missing mass to the four charged final state particles (MM^2) for the reactions $\pi^- p \rightarrow p\pi^-\pi^-\pi^+$(a) and $\pi^- p \rightarrow p\pi^-\pi^-\pi^+\pi^o$(b) are shown for 12 and 8 GeV/c in fig. 9. The good separation between the MM^2 for reactions (a) and (b) on the one hand and the threshold of multineutrals ($2\pi^o$) on the other hand demonstrates that it will not be difficult to separate between different channels. (In this context the OMEGA is about a factor 2 more accurate than the 2 metre H.B.C.)

CERN/D.Ph.II/PHYS 70-66
1.12.1970

5. MEASURABILITY

By tracing each particle through the spark chamber plate system with all the plates perpendicular to the beam direction it was found that essentially all events would be measurable. This is due to the fact that at high incident energies and relatively small M_x - the charged pions all go forward in the laboratory system with relatively small angles. The slow proton, which could be a source of trouble, is constrained by the trigger to have a good geometry for measurement in the chambers.

6. CONCLUSIONS

The proposal investigates the possibility of studying charged non-strange boson resonances in a selected mass region (for example (1.5 - 2.0) GeV/c^2) using a time of flight trigger on the recoil proton.

Full information on the charged decay products can be obtained in the OMEGA spark chamber array and should allow a more detailed study of the boson resonance spectra in this region than has up to now been possible.

Good mass resolution, $\pm$ (10 - 14) MeV, and the high statistics obtainable (120,000/day or ~100 times present day H.B.C. statistics) in a restricted mass interval are other particular characteristics of the proposed experiment.

7. PROPOSAL

We propose a run of at least 10^6 good photographs which should be achievable within a 10 day P.S. period using a beam of 12 GeV/c momentum .

CERN/D.Ph.II/PHYS 70-66
1.12.1970

COMMENT

a) It is hoped that such a run will be complementary to a similar run using a neutron trigger so that the physics of I = 0 and I = 1 bosons could be extracted via a comparison of the two experiments.

b) This trigger could be considered as a general facility for other experimental proposals e.g. Λ^o trigger and electromagnetic decay trigger.

APPENDIX 1

Trigger

a) General Considerations :

The triggering principle, though similar to well known missing mass techniques, has some novel features which are either allowed or imposed by the OMEGA Configuration. As is well known, for two body interactions such at $\pi^- p \rightarrow p X^-$, knowledge of the proton's final momentum and angle determines the missing mass X^- and its momentum transfer (figs. 1a and 1b). In the classical missing mass experiment[1] the inaccuracy in M_X due to inaccurate momentum measurement is made small by a properly restricted choice of the momentum region, the so called Jacobian peak region. The proton angle is measured accurately and the momentum is restricted by rough measurement to this region. However, in the proposed experiment M_x and Δ^2_x are reconstructed from the secondary tracks observed in the spark chambers, and apart from possible on-line estimates of M_x and Δ^2_x the trigger serves only to select interesting regions of the $(p - \theta)$ plane, or equivalently, the $(M_x - \Delta^2_x)$ plane. There is therefore no need for restriction to a small region of mementum transfer.

Referring to figure 2a we see that the OMEGA magnet synchronises all protons corresponding to a given mass by an approximate cyclotron principle. Such a group of protons form in fact what may be conveniently thought of as a "wave" rotating about the interaction point. Different values of M_X, as explained above, correspond to different arrival times of the wave at a given position. We note that waves corresponding to smaller values of M_x arrive later and also that the position of the proton along the "wave-front" depends monotonically, for all M_x, on the proton momentum

(which determines Δ_x^2). Therefore, a counter placed (for example) at a position AB on fig. 2b will be struck at a time which depends on M_x and at a position which depends on Δ_x^2. This is the basis of the triggering method.

Normally one could measure the position x and time t at the surface of the counter by using two tubes, one at each end. Addition and subtraction of the arrival times of signals at each end would then give analogues of x and t. This is, however, impractical owing to the difficulty of shielding the phototube at B. Therefore we propose to use only one phototube at A (and to measure the position, if required for on-line checking, by means of a wire chamber). The time measured will then no longer be the time of arrival of the proton at the surface of the counter, but the time of the phototube output pulse. In this case (with the scintillator at AB) the coordinate transformation T : $(t,x) \rightarrow (M,\Delta^2)$ between the measured quantities (t,x) and those which are of physical interest is shown in fig. A 1.1.

Clearly, a trigger on signals within a rectangular t - x region would have the property that the selected Δ^2 and M_x regions would be strongly correlated. A better solution (which also makes the tube at A easier to shield), is obtained by rotating the counter to a new position CD. Effectively, this compensates to first order the transit time of light from protons of different momenta, by giving those with a shorter transit time a longer flight path to the counter. The resulting transformation $(t,x) \rightarrow (M,\Delta^2)$ is shown in fig. A 1.2. In general, we note that there will exist a coordinate transformation $(t,x) \rightarrow (M\Delta^2)$ for every position of the counter. Fig. A 1.3 shows the transformation for a counter position having the property that the rectangular "bite" in the (t,x) system defines an almost rectangular bite in the (M,Δ^2) system at 12 GeV/c incident pion momentum.

Finally we point out that an exact knowledge of the transformation T is necessary to specify the effect on an arbitrary $d^2\sigma/dMd\Delta^2$ distribution of the triggering system for a given counter position. This must be known to achieve meaningful angular and mass distributions. We would therefore perform detailed preliminary measurements on the properties of the T.O.F. counter, possibly using the 600 MeV synchrocyclotron to simulate the recoil protons, in order to check the precise form of the transformation which depends among other things on the effective light velocity in the scintillator and on the triggering electronics. The optimum counter position would also, of course, depend on these factors, the position indicated in fig. 2 being based on calculation and not measurement.

b) Rejection of pions, counter configuration

As indicated in the main text of the proposal (Fig. 4) the time of flight separation between pions and protons coming from the target will enable the t-counter to be delayed so as to accept only very few pions. However, in order to increase the overall redundancy we propose a further rejection factor for pions by including an absorber after the t-counter T_1 (fig. A 1.4) which is thick enough to stop those protons which do not already stop in the t-counter. Pions will continue through the absorber to be counted in T_2. The t-counter will also be preceded by a thin counter to prevent T_1 tube noise counts from giving false triggers. Thus, the logical requirement $To \cdot T_1 \cdot \bar{T}_2$ will be needed before a count will be accepted.

This arrangement will also help to reduce the background of charged particles in the T.O.F. counter, consequently the random coincidences will also be reduced. A veto counter will be located at the end of the optical chambers to reduce the random coincidence rate still further (see below). The full logical requirement will therefore be (with beam counter(s) B): $B \cdot \bar{A} \cdot To \cdot T_1 \cdot \bar{T}_2$

c) Random coincidences

While it is never possible to estimate the proportion of random coincidences in an experiment owing to lack of realistic information about backgrounds etc., we believe it is useful to point out what would probably be the most serious sources of random coincidence with the apparatus described above, under various assumptions concerning background rates and operating conditions.

We define by "Random Coincidences" any combination of events which falsely satisfies the logical requirements for triggering the spark chambers. These will of course, include combinations of tube noise, background counts, nuclear interactions in scintillators or counters, wrappings in the beam etc. etc. etc.

We start by assuming a simplified trigger requirement consisting of

1) a beam count
2) absence of a count in the veto counter A
3) a count in t-counters T_1 T_0 (but without the T2 veto) See fig. A 1.4.

We also make some assumptions about running conditions.

a) Rate (N_0) 2 x 10^5/burst [10^6/sec - see (6)]
b) Spill (s) 200 ms, no fine structure, bad spills detected and vetoed.
c) Beam counts are free of RC(Random Coincidences). Thus counter B is considered as a single counter, though there may be other in coincidence with it upstream.
d) Gate $\pm$ 5 n.s. derived from B applied to the T.O.F. counter T_1. Call this resolving time $\pm \tau$
e) Anticoincidencing of straight through beams by A.
f) All counts in T_1 go through T_0. We call $T \equiv T_1 \cdot T_0$

f will not be very close to 1 because of nuclear interactions etc. : in the absorber. However, f = 0.9 is not too pessimistic; we then obtain R = 0.10/burst.

It must be stressed that this is only an estimate the most important factor is K. If k ~5 °/o (rate $N_{\bar{T}.\bar{A}.\bar{B}}$ = 10000/burst) R would be 0.5/burst. k will depend on neutron fluxes, shielding, neighbouring experiments etc. Current estimates for unshielded muon background flux in the West area indicate ~2 x 10^3 per sq. m./steradian/burst, which would give $N_{T.\bar{A}.\bar{B}.}$ ~ 4 x 10^4, and R = 2/burst. Shielding should bring this down by a factor ~ 10.

d) Possibility of on-line information

It would be useful to assess on line the nature and quality of the data being accepted during the experiment. We are at present studying the feasibility of this. Naturally, some additional equipment would be necessary. One possibility would be to measure not only the proton time of arrival at CD but also its position. The position and time measurements could then be displayed to allow the physicist to decide where each event lay relative to the curvilinear coordinates (M, Δ^2) of figs. A 1.1 - A 1.3 . We see from inspection that only approximate information on x is necessary. The plots A 1.1 - A 1.3 are relatively insensitive to the position of the interaction point in the hydrogen target. Should an estimate of this point be necessary, the method suggested by the neutron trigger group for the same purpose would be perfectly adequate. This method requires two Charpak Chambers sandwiched between optical chamber units, the interaction point being estimated from the configuration of the wires touched.

We would, therefore, as part of the preliminary investigations referred to in (a) above, measure the accuracy in time of flight information between a small beam counter and the t-counter. With care, we can expect a "start-time" accuracy of $\pm$ 35 P.S. (Bollini et al.13). The "stop" accuracy would of course be much worse, but

We now calculate what would appear to be the most serious contribution to RC - that coming from coincidences B 0 T 0 $\bar{A}$.

Rate of B = $N_{B.\bar{A}.\bar{T}}$ (by supposition (e))

Rate of T = $N_{T.\bar{A}.\bar{B}}$

$$R = 2\tau N_{B.\bar{A}.\bar{T}} \cdot N_{T.\bar{A}.\bar{B}} \cdot \frac{1}{S}$$

Assume : $N_{T.\bar{A}.\bar{B}} = kN_o$

for example k = 1 $^o/_o$ gives $N_{T.\bar{A}.\bar{B}}$ = 2000/burst for $N_o = 2.10^5$
What is $N_{B.\bar{A}.\bar{T}}$? The main part is probably from events occuring in the target (scattering out of A).

σ_T(8 GeVπ^-p) = 28 mb.

$N_{B.\bar{A}.\bar{T}} = N_o \sigma_T L$ (L = length of target in feet)

So $R = 2\tau kNo\sigma_T L / s$

$R = 2\tau No^2(k\sigma_T L)/s$

To allow further contributions to $N_{B.\bar{A}.\bar{T}}$ from non-target material in the beam we can increase σ_T to 50 mb for the purposes of calculation. Thus for $2\tau = 10^{-8}$ sec, $N_o = 2.10^5$, $k = 10^{-2}$, $\sigma_T = 50.10^{-3}$

L = 1 foot, s = 1/5

$R = 10^{-8} x (4.10^{10}) x 10^{-2} x (50 . 10^{-3}) x 1 x 5$

R = 1.00/burst

We now include the requirement $\bar{T}_2$. This will give R another factor ≤ 1 depending on how efficient T_2 is.

$$\frac{N_{T.\bar{A}.\bar{B}.\bar{T}_2}}{N_{T.\bar{A}.\bar{B}.}} = (1 - f)$$

Then : $R = 2\tau N_{B.\bar{A}.\bar{C}.} \cdot N_{T.\bar{A}.\bar{B}.\bar{T}_2} \cdot 1/5$

$$R = 2\tau . No^2 . \frac{k\sigma_T L}{s} . (1 - f)$$

with proper optical design, good photon statistics, fast tubes such as the R.C.A. 4522 and careful electronic processing (zero crossing) one can probably achieve $\pm$ 350 p.s. (Bollini et al. 14) Together with position measurement on the T.O.F. counter to $\pm$ 1 cm and interaction point accuracy of $\pm$ 2.5 cms, we see from inspection of figs. A 1.1 to A 1.3 that mass accuracies between $\pm$ 25 and $\pm$ 50 MeV (depending on M_x, Δ_x^2 and incident momentum) could be achieved. This should be sufficient to give some feeling as to the general characteristics of the information being gathered.

Clearly, further detailed studies should be made before deciding whether or not useful on-line information can be obtained.

APPENDIX 2

Evaluation of errors

To have an estimation of the errors we can expect on the quantities of most interest in our experiment, we have traced the triggered events in the OMEGA spark chamber system taking into account the main features of the apparatus.

a) Errors due to optical spark chambers :

Errors on the geometrical quantities $1/\rho, \lambda, \Phi$, for each track, have been calculated following the procedure described in Ref. 12, which has been shown to be meaningful in handling events occuring inside optical spark chambers systems placed in a magnetic field.

The variance matrix error elements which were used for $1/\rho$, λ, Φ are :

i) Setting errors :

$$c_{11} = \sigma^2_{1/p} = \left(\frac{8\ (\overline{\Phi^2})}{L^2 \cos^2\lambda} \right)^2$$

$$c_{12} = c_{21} = c_{23} = c_{32} = 0.$$

$$c_{22} = \sigma^2_{\lambda} = \left(\frac{6\ (\overline{\Phi^2})}{L} \right)^2 (\cos^2\lambda + 0.01) \qquad (1)$$

$$c_{13} = c_{31} = \langle \sigma_{1/\rho} \sigma_{\Phi} \rangle = -32\ \frac{\sigma^2 (\overline{\Phi^2})}{L^3 \cos^2\lambda}$$

$$c_{33} = \sigma^2_{\Phi} = \left\{ \frac{4\ \sigma (\overline{\Phi^2})}{L \cos\lambda} + \sigma_{1/\rho}\ (x_B - x_V) \right\}^2$$

ii) Multiple scattering errors in the optical chambers

$$c_{11} = \sigma^2 1/\rho = \frac{2}{3}\cdot\left(\frac{21}{\rho}\right)^2 \cdot \frac{1}{LL_o} \cdot \frac{1}{\cos^2\lambda}$$

$$c_{12} = c_{21} = c_{23} = c_{32} = 0.$$

$$c_{22} = \sigma^2_\lambda = \frac{1}{6}\cdot\left(\frac{21}{\rho\beta}\right)^2 \frac{L}{L_o} \qquad (2)$$

$$c_{13} = c_{31} = <\sigma 1/\rho\ \sigma_\Phi = \frac{1}{\sqrt{12}}\left(\frac{21}{\rho\beta}\right)\frac{1}{\sqrt{L_o}} \quad \frac{1}{\cos^{3/2}\lambda}$$

$$c_{33} = \sigma^2_\Phi = \frac{1}{12}\left(\frac{21}{\rho\beta}\right)^2 \cdot \frac{L}{L_o} \quad \frac{1}{\cos^3\lambda}$$

Where the symbols used are defined as follows :

ρ = radius of curvature (cm), λ = dip angle (radians)
Φ = angle in x y plane with incident (radians)
L = length of track (cm)
x_B = coordinate of the first spark (cm)
x_V = coordinate of the vertex, σ = setting error (cm)
p = momentum (MeV/c), L_o = radiation length of optical chambers (cm)

To take account of the anisotropy of the optical spark chamber system, each track was followed until it formed a maximum angle of 60^o with the normal to the plates and the setting error for a track was given by (12)

$$\sigma^2(\overline{\Phi^2}) = 0.020 + 0.17\ \overline{\Phi^2}\ (\text{cm})$$

where Φ^2 is the mean of the squared angle formed by the track with the plates.

b) Errors due to the target :

We have considered a hydrogen vessel 20 cm long and of diameter $\emptyset$ = 2 cm. The interaction points were uniformily distributed in the beam direction (x) and had a gaussian density in the transverse directions ($\bar{y}$ and $\bar{z}$). The vacuum tank was schematized with a cylinder of $\emptyset$ = 4 cm. and a thickness equivalent to 2 mm of Mylar. The side of the target through which the protons exit consists of a mylar window .3 mm thick. The error variance matrix due to multiple scattering in hydrogen and mylar on λ and Φ angles are, as usual, given by :

$$C(2,2) = C(3,3) = \left(\frac{15}{\rho\beta}\right)^2 \left(\frac{L_H}{L_{o_H}} + \frac{L_{My}}{L_{o_{My}}}\right) \qquad (3)$$

$$C(1,1) = C(1,2) = C(2,1) = C(3,1) = C(1,3) = C(3,2) = C(2,3) = 0$$

where : L_H, L_{My} = path of the particle in hydrogen and mylar (cm)

L_{o_H}, $L_{o_{My}}$ = radiation length of hydrogen and mylar (cm)

This matrix has been added to the measurement and multiple scattering matrix error.

c) Optimum measured length for the proton :

We are mainly interested in the MM to the recoil triggered proton. Since we trigger mainly in the Jacobian region the error on the MM comes predominatly from the error on Φ of the proton. ($\lambda \sim o$). Since the setting error on Φ decreases with the measurement length like $\frac{1}{L}$ while the scattering error increases like $\sqrt{L}$ there exists an optimum length which mimimizes the error on Φ.

$$L_{OPT}^{3} = \frac{128}{147} \sigma^2 L_o \rho^2 \beta^2 \quad (\lambda = 0) \qquad (4)$$

We have used the full usefull length of the track to calculate the error on $1/\rho$, and the optimised length to calculate the errors on Φ and λ.

d) Propagation of errors :

Starting from the described variance matrix in $(1/\rho, \lambda, \Phi)$ errors on several quantities of physical interest have been calculated with the standard matrix error propagation formalism.

Discussion on the results obtained is given in the text.

REFERENCES

1) M.N. Focacci, W. Kienzle, B. Levrat, B.C. Maglic and M. Martin Phys. Rev. Letters, 17, 890 (1966).

2) A. Astier, Rapporteurs talk on mesons to the KIEV Conference on High Energy Particle physics (1970).

3) R.H. Dalitz, International Conference on Symmetries and Quark Models Wayne State University (1969).

4) C. Quigg and F. von Hippel International Conference on Meson Spectroscopy, Philadelphia (1970).

5) H. Goldberg, Phys. Rev. Letters 21, 778, (1968).

6) The quoted cross-section is aninterpolation from existing data at other energies. The number of events in the peak is taken (as an example of typical values) from : Bartsch et al Nucl. Phys. B22, 109, (1970) $\pi^+ p \rightarrow p g^+$ at 8 GeV/c.

7) Caso et al Nuovo Cimento 54A, 983 (1968).

8) Caso et al.Lettere Nuovo Cimento 2 437 (1969).

9) Ioffredo et al. Phys. Rev. Letters 21, 1212 (1968).

10) Kramer et al. Phys. Rev. Letters 25, 396 (1970).

11) Caso et al. Lettere Nuovo Cimento 3, 707 (1970).

12) P. Astbury et al. Nuclear Instruments and Methods 46, 61 (1967) P. Mühleman and J.D. Wilson CERN 70-17 (1970).

13) Bollini et al. Nucelar Instruments and Methods 81(1970) 56.

14) Bollini et al. Nuovo Cimento X, Vol. 61A, pp. 125 - 172.

TABLE 1a - $\pi^+ p \rightarrow p x^+$ at 8 GeV/c

Reaction	σ (μb)	o/o triggered	σ trigger (μb)	Kilo events/10^6 ev.
$\pi^+ p \rightarrow p\pi^+\pi^o$	580	1.1	6.5	183
$p\pi^+ x^o$	2,500	1.12	28.0	357
$p\pi^+\pi^+\pi^-$	1,500	1.17	17.6	225
$p\pi^+\pi^+\pi^-\pi^o$	1,800	.84	15.1	193
$p\pi^+\pi^+\pi^- x^o$	2,000	.41	8.2	105
$p\pi^+\pi^+\pi^-\pi^+\pi^-$) $p\pi^+\pi^+\pi^-\pi^+\pi^-\pi^o$) $p\pi^+\pi^+\pi^-\pi^+\pi^- x^o$)	1,500	.2	3.0	37
	9,880		78.4	1,000

TABLE 1b - $\pi^- p \rightarrow p x^-$ at 11.2 GeV/c

Reaction	σ (μb)	o/o triggered	σ trigger (μb)	Kilo events/10^6 ev.
$\pi^- p \rightarrow p\pi^-\pi^o$	700	.67	4.7	100
$p\pi^- x^o$	1,400	.67	9.4	200
$p\pi^+\pi^-\pi^-$	1,200	.96	11.5	245
$p\pi^+\pi^-\pi^-\pi^o$	1,200	.63	7.6	162
$p\pi^+\pi^-\pi^- x^o$	2,500	.42	10.5	225
$p\pi^+\pi^+\pi^-\pi^-\pi^-$	600	.42	2.5	53
$p\pi^+\pi^+\pi^-\pi^-\pi^-\pi^o$) $p\pi^+\pi^+\pi^-\pi^-\pi^-\pi^- x^o$)	2,400	.03	.7	15
	10,000		46.9	1,000

TABLE 2

Resonance or peak	Technique	Incident momentum (GeV/c)	Reference	Cross-section (μb)	Nb. of events over backgr.	Signal/Backgd.	Nb. of events(*) over background expect. in Ω
R_1 (1630)	MMS	7 ÷ 12	1	26	370	1/4.7	11,500
R_2 (1700)	MMS			32	270	1/3.3	17,000
R_3 (1750)	MMS			36	340	1/3,5	23,000
S (1930)	MMS	12	1	32	230	1/7	26,000
g (1650) → 2π	HBC	12	6	20	120	1/1,5	9,000
ρ (1700) → 4π	HBC	11.2	7	50	100	1/2	31,000
A_3 (1640)	HBC	11.2	8	58	100	1/3	22,000
	HBC	13.	9	41	40	1/2	
S → 2π	HBC	13.	10	7	30	1/1,5	5,000
S → 4π	HBC	11.2	11	19	30	1/2	15,000

(*) assuming 10^6 total events

TABLE 3a

$-t$ p/p $(GeV)^2$	σ_{Φ_p} (mrad)	σ_{M_x} (MeV)									
		TOTAL	SETTING	SCATT IN Ch.	SCATT IN H	SCATT IN My	INCIDENT	INCIDENT ΔP_i ONLY	INCIDENT $\Delta\theta_i$ ONLY	$\sigma_{M(2\pi)}$	$\sigma_{M(3\pi)}$
.1	10.	18.	6.	12.	6.	8.	3.5	2.7	2.2	5.5	8.5
.25	5.5	13.	5.	8.	4.	5.	4.5	3.3	3.	5.5	8.5
.40	4.	10.	4.5	6.	3.	3.5	4.5	3.3	3.	5.5	8.5

PARAMETERS : P_i = 12 GeV/c ; $\frac{\Delta P_i}{P_i}$ = 0.3°/o ; $\sigma_{\Phi_i} = \sigma_{\lambda_i}$ = 1 mrad.

Target : Length = 20 cm $\emptyset$ = 2cm.
Proton Window = .03 cm (Mylar)
Vacuum Tank = .2 cm (Mylar)
Setting Error = .02 + .17 $\langle\bar{\Phi}^2\rangle$ cm.

TABLE 3b

$-t$ p/p $(GeV)^2$	σ_{Φ} p (mrad)	σ_{M_π} (MeV) TOTAL	SETTING	SCATT IN Ch.	SCATT IN H	SCATT IN My	INCIDENT	INCIDENT ΔP_i ONLY	INCIDENT $\Delta\theta_i$ ONLY	$\sigma_{M(2\pi)}$	$\sigma_{M(3\pi)}$
.10	10.	13.	5.	10.	4.	5.	2.5	2.2	1.	5.2	7.5
.25	5.	9.5	4.	6.	3.	4.	3.5	3.0	1.8	5.2	7.5
.40	4.	7.	3.	4.	2.	3.	3.5	3.0	1.8	5.2	7.5

PARAMETERS : $P_i = 8$ GeV/c ; $\frac{\Delta P_i}{P_i} = 0.3\%$; $\sigma_{\Phi_i} = \sigma_{\lambda_i} = 1$ mrad.

Target : Length = 20 cm $\varnothing$ = 2 cm.
Proton Window = .03 cm. (Mylar)
Vacuum Tank = .2 cm. (Mylar)
Setting error = .02 + .17 $\langle\bar{\Phi}^2\rangle$ cm.

CERN/D.Ph.II/PHYS 70-66
1.12.1970

FIGURE CAPTIONS

1) a) Plot of θ_{Lab} against p_{Lab} for proton in the reaction $\pi p \rightarrow pX$ at 12 GeV/c. The curves are for different values of the recoiling mass M_X. Also shown are the curves of C.M. production angle. The triggered region is shaded.

   b) Same as 1a at 8 GeV/c.

2) a) Sketch of the OMEGA apparatus with the drawing of proton trajectories for $M_X = 1.7$ GeV/c^2 and p in the range 0.3 - 0.7 GeV/c. See text.

   b) Same as 2a, with the original position of the counter for $M_X = 1.7$ and $\tau = 25$ ns (dashed, A) and the position after rotation (full line, CD), as explained in App. 1.

3) Plot of time of arrival of protons at the counter against M_X. The events are generated by Montecarlo method at 12 GeV/c.

4) Distribution of time of arrival of protons and pions at the counter.

5) a) Acceptance of the triggering system as function of recoiling mass (M_X).

   b) Acceptance as function of momentum transfer ($-t_{p/p}$).

6) Plot of momentum transfer versus M_X for a sample of 4-p events $\pi^- p \rightarrow pX^-$ at 11.2 GeV/c. Mass and -t total distributions are also shown, along with the triggered region (shaded areas).

7) a) Scatter plots of the various contributions to the error on M_X as functions of momentum transfer at 12 GeV/c.

   b) Same as 7a at 8 GeV/c.

8) Distributions of errors on 2π and 3π effective mass.

9) Squared missing mass for reactions $p\pi^+\pi^-\pi^-$ and $p\pi^+\pi^-\pi^-\pi^o$.

FIGURE CAPTIONS CONTINUED

A 1.1 Coordinate transformation $(t,x) \rightarrow (M,\Delta^2)$ at $P_i = 8$ GeV/c for position AB of fig. 2b.

A 1.2 Coordinate transformation $(tx) \rightarrow (M,\Delta^2)$ at $P_i = 8$ GeV/c for position CD fo fig. 2b.

A 1.3 Coordinate transformation $(t,x) \rightarrow (M,\Delta^2)$ at $P_i = 12$ GeV/c for position CD of fig. 2b.

A 1.4 Layout of counters and absorber.

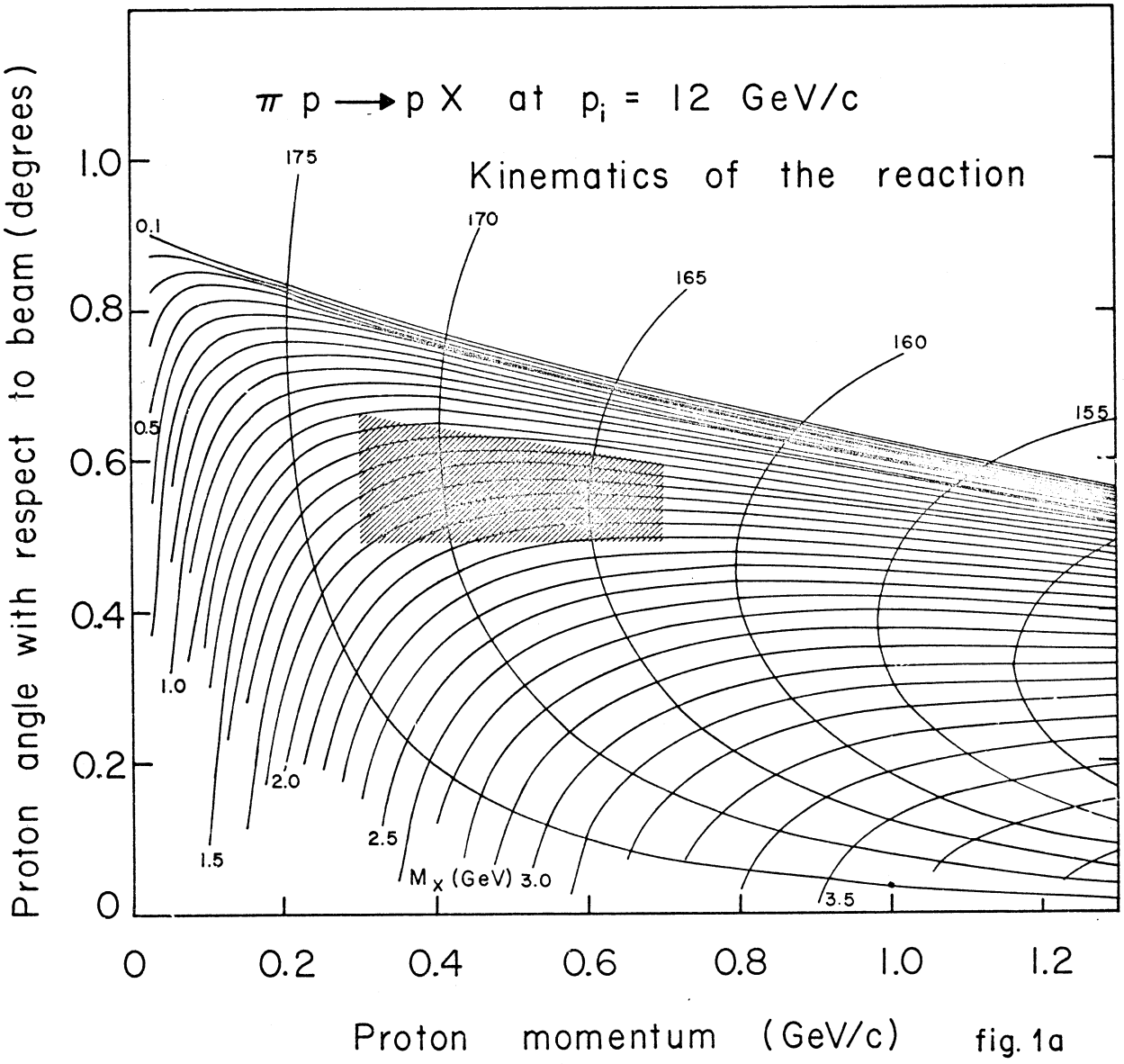
π p ⟶ p X at p_i = 12 GeV/c
Kinematics of the reaction
Proton angle with respect to beam (degrees)
Proton momentum (GeV/c)
0
0.2
0.4
0.6
0.8
1.0
1.2
175
170
165
160
155
0.1
0.5
1.0
1.5
2.0
2.5
3.0
3.5
M_X (GeV)

fig. 1a

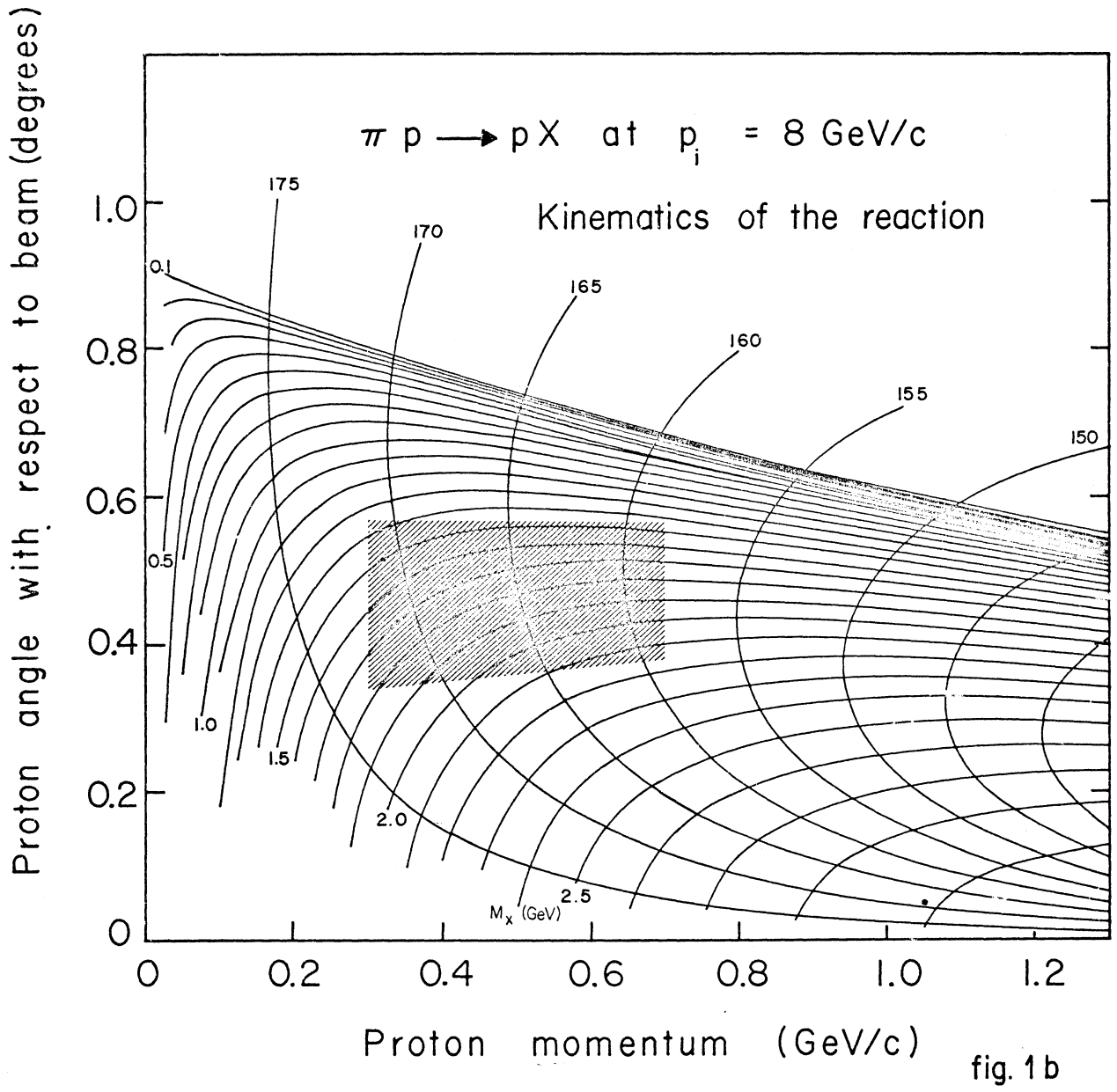
π p ⟶ pX at p_i = 8 GeV/c
Kinematics of the reaction
175
170
165
160
155
150
0.1
0.5
1.0
1.5
2.0
2.5
M_X (GeV)
Proton angle with respect to beam (degrees)
Proton momentum (GeV/c)
0
0.2
0.4
0.6
0.8
1.0
1.2

fig. 1b

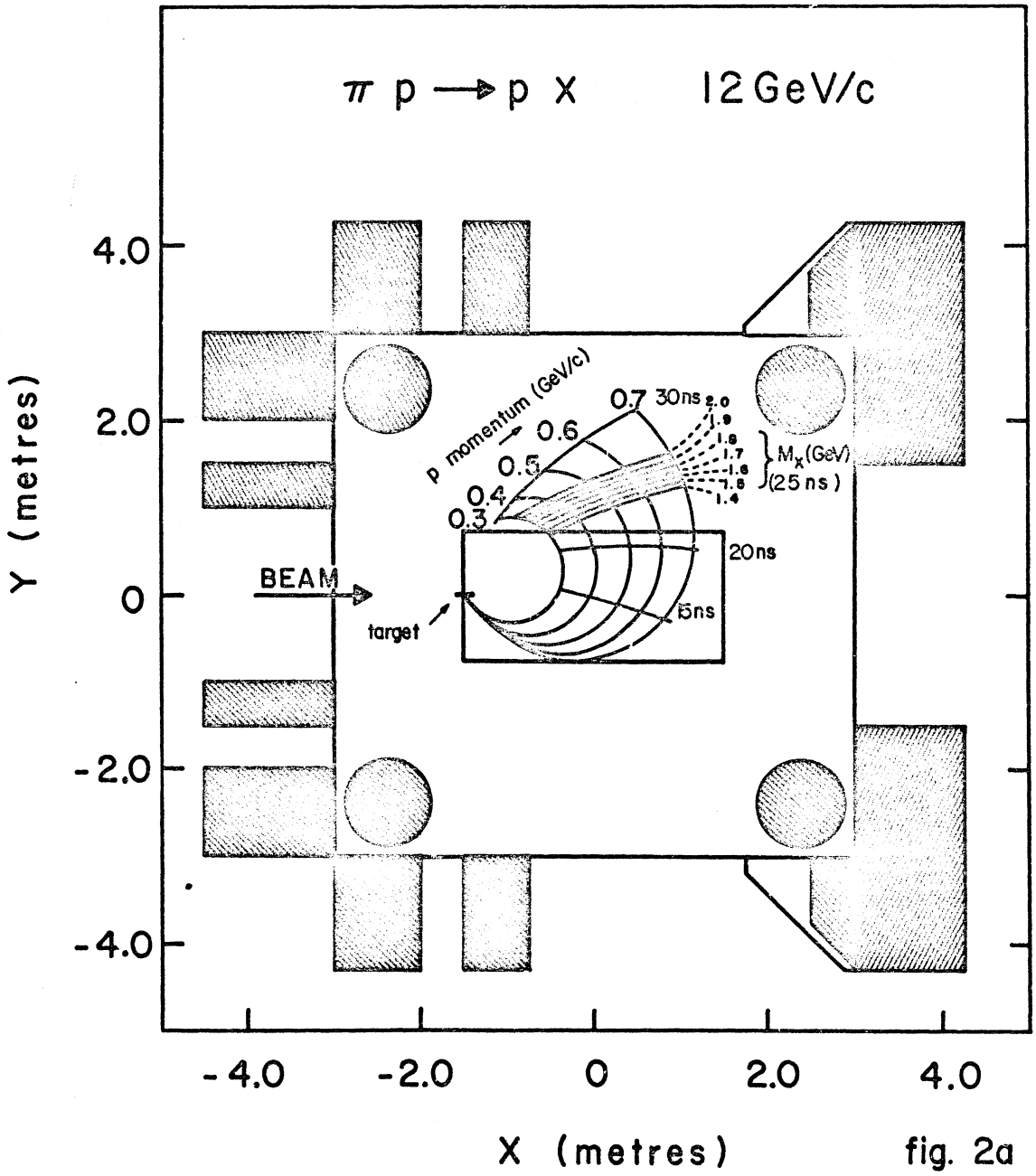
π p → p X 12 GeV/c
4.0
2.0
0
-2.0
-4.0
Y (metres)
-4.0
-2.0
0
2.0
4.0
X (metres)
BEAM
target
p momentum (GeV/c)
0.7
0.6
0.5
0.4
0.3
30ns
20ns
15ns
M_X(GeV)
(25 ns)

fig. 2a

Layout of the apparatus

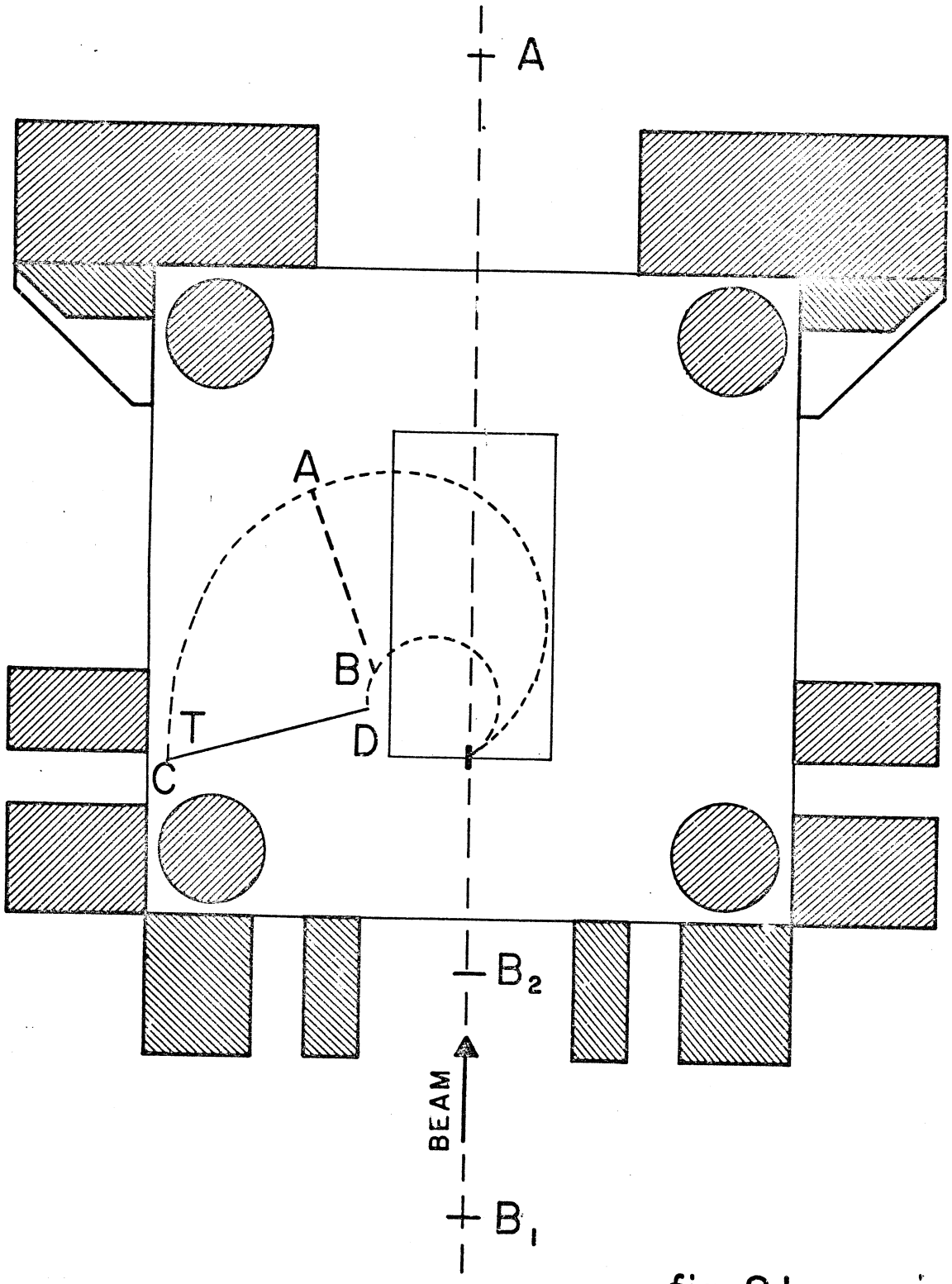

fig. 2b

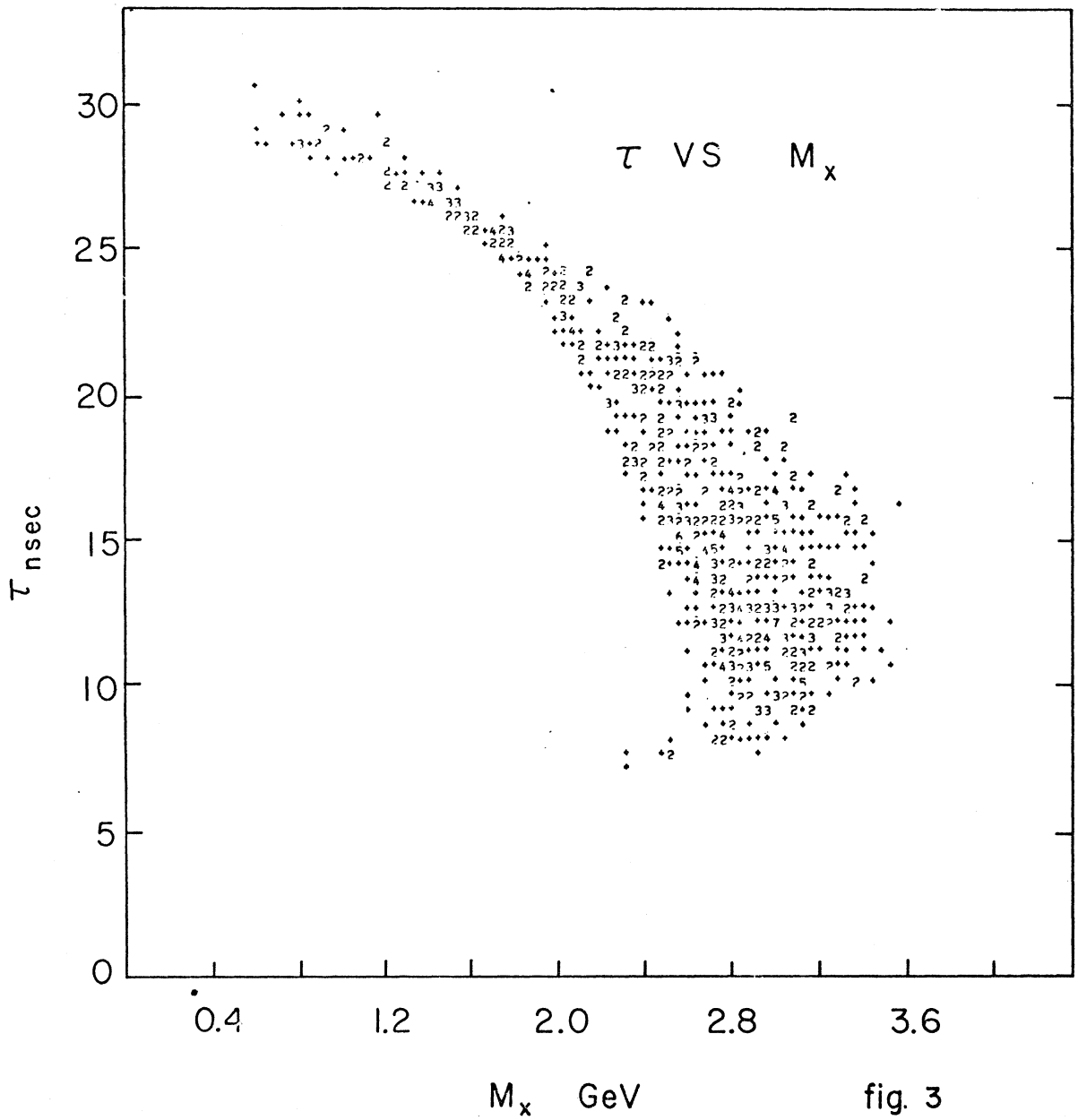

fig. 3

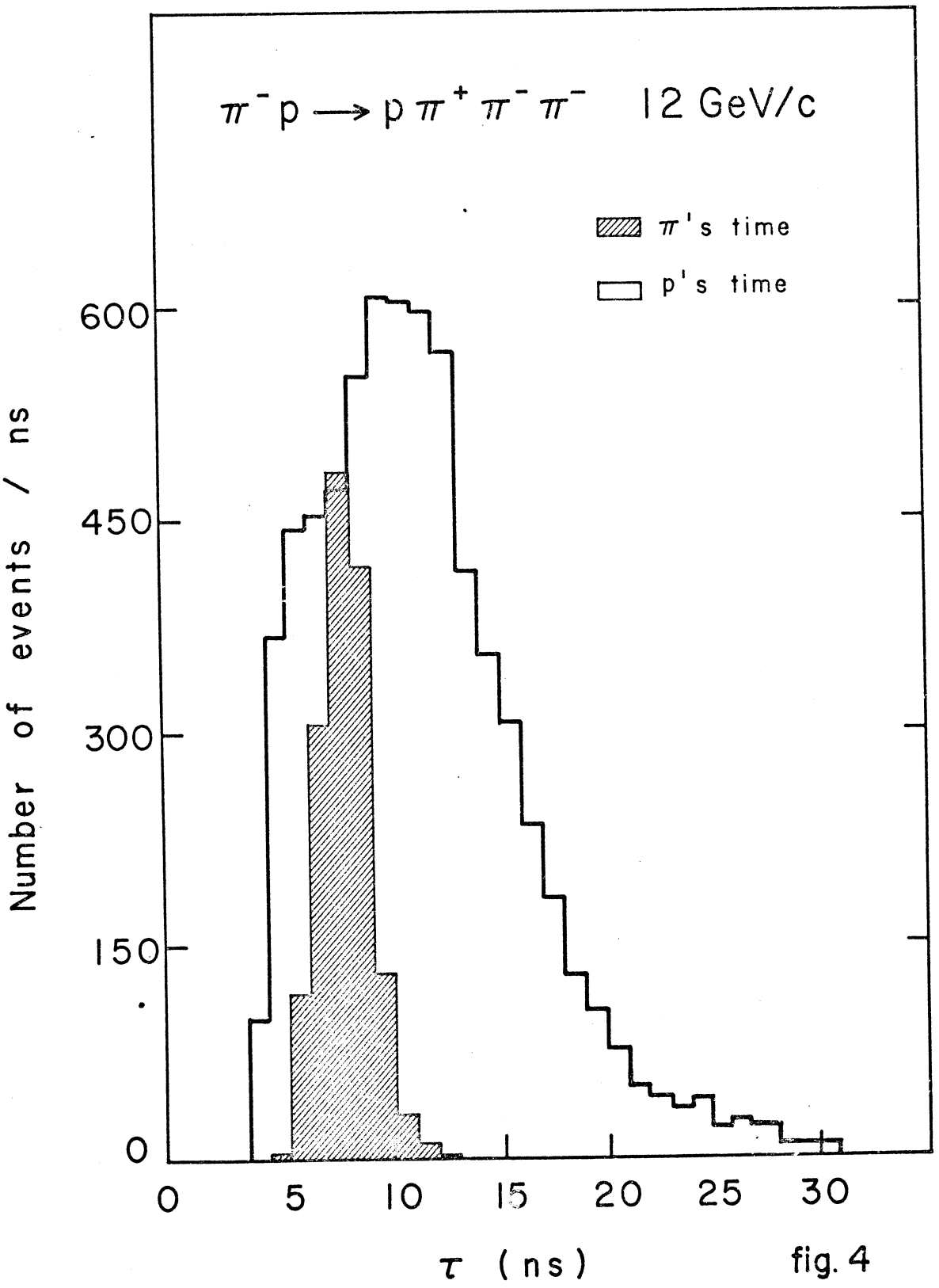
$\pi^- p \longrightarrow p\,\pi^+\,\pi^-\,\pi^-$ 12 GeV/c
π's time
p's time
Number of events / ns
600
450
300
150
0
0
5
10
15
20
25
30
τ (ns)

fig. 4

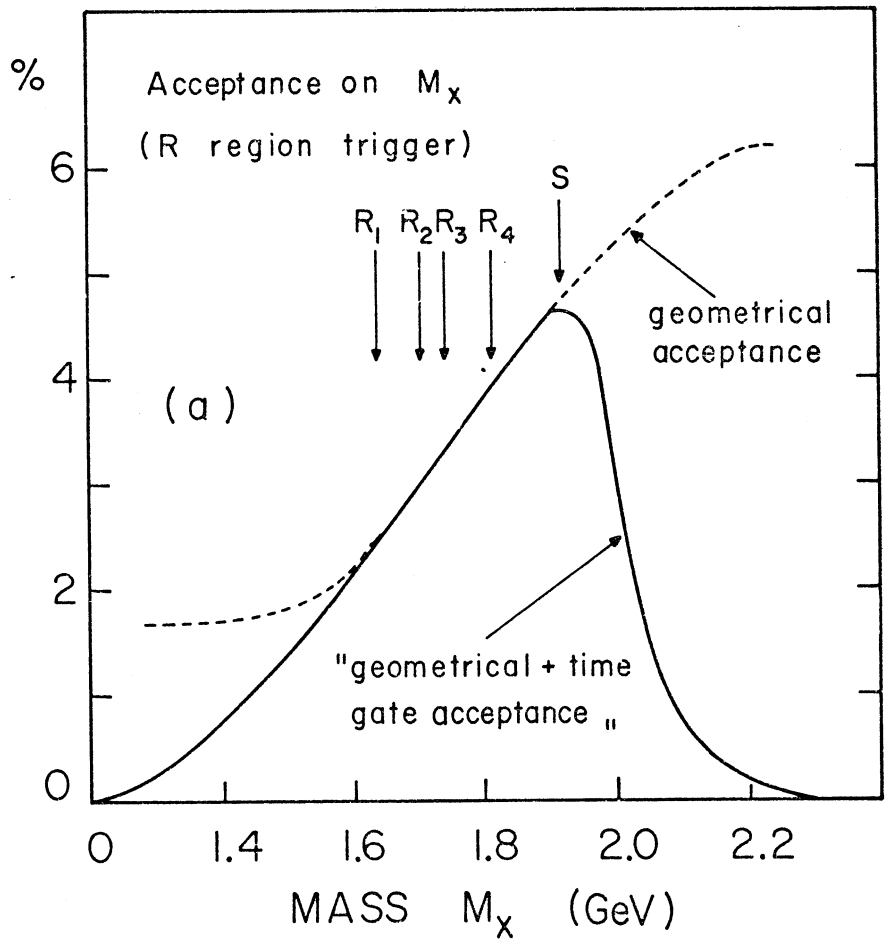
%
Acceptance on M_X
(R region trigger)
S
R_1 R_2 R_3 R_4
geometrical acceptance
(a)
"geometrical + time gate acceptance"
6
4
2
0
0
1.4
1.6
1.8
2.0
2.2
MASS M_X (GeV)

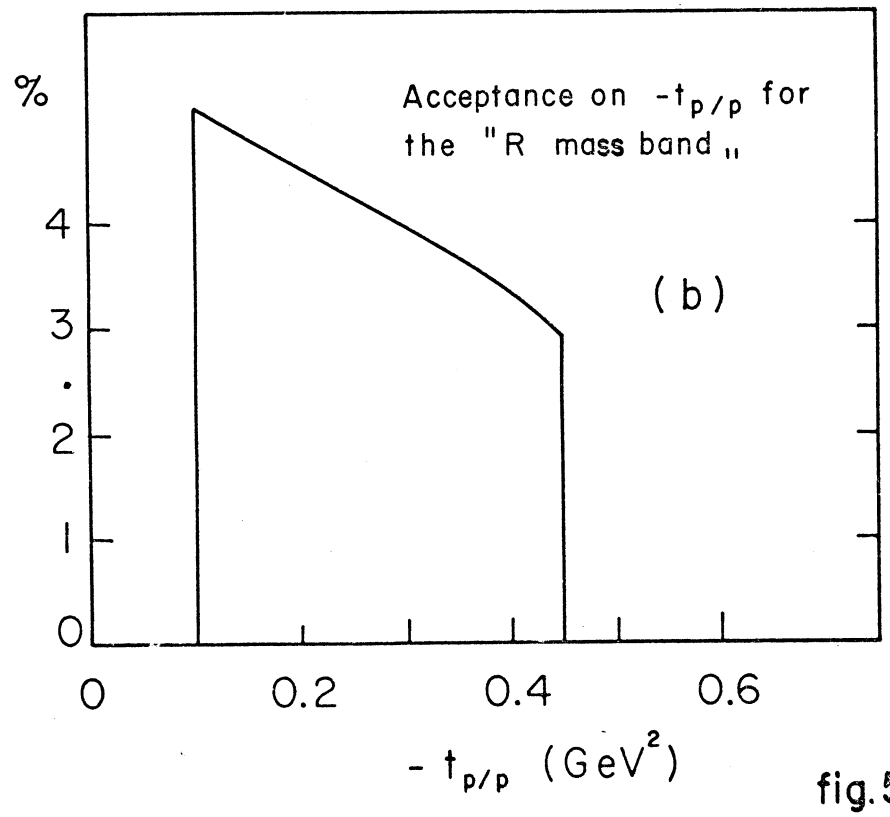
%
Acceptance on $-t_{p/p}$ for the "R mass band"
(b)
4
3
2
1
0
0
0.2
0.4
0.6
$-t_{p/p}$ (GeV^2)

fig.5

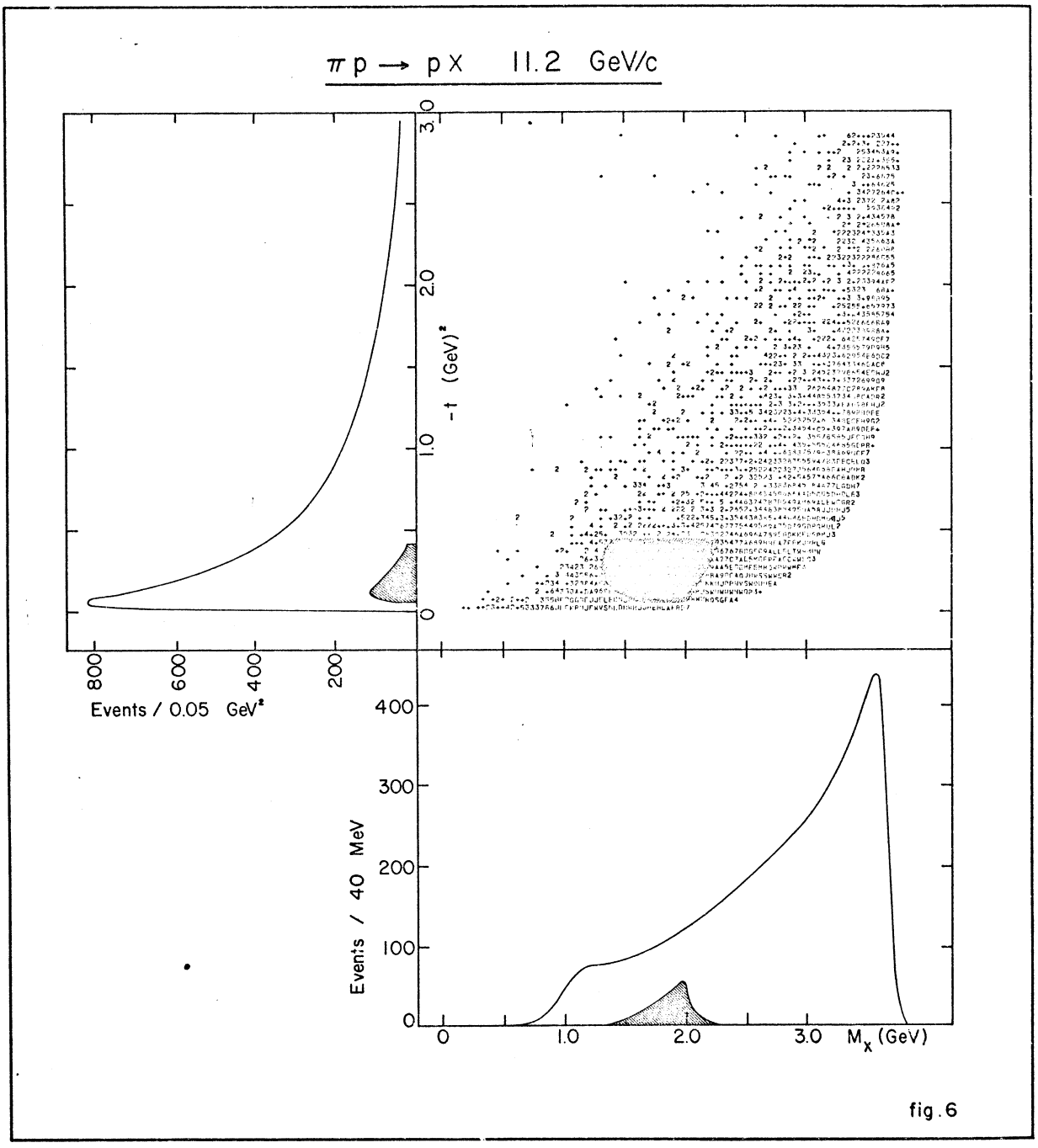

fig. 6

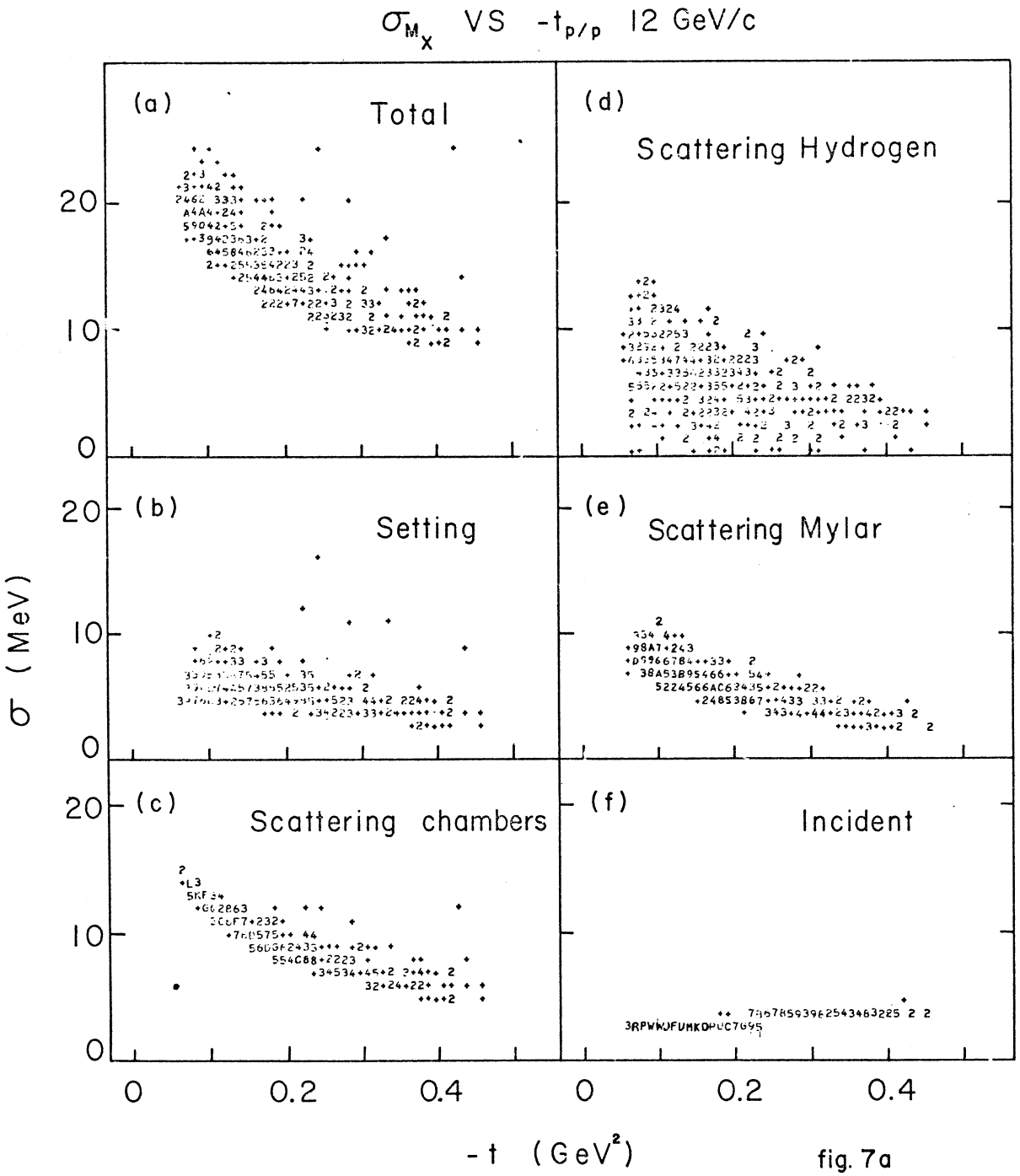
σ_{M_X} VS $-t_{p/p}$ 12 GeV/c
(a) Total
(d) Scattering Hydrogen
(b) Setting
(e) Scattering Mylar
(c) Scattering chambers
(f) Incident
σ (MeV)
0
10
20
0
0.2
0.4
$-t$ (GeV^2)

fig. 7a

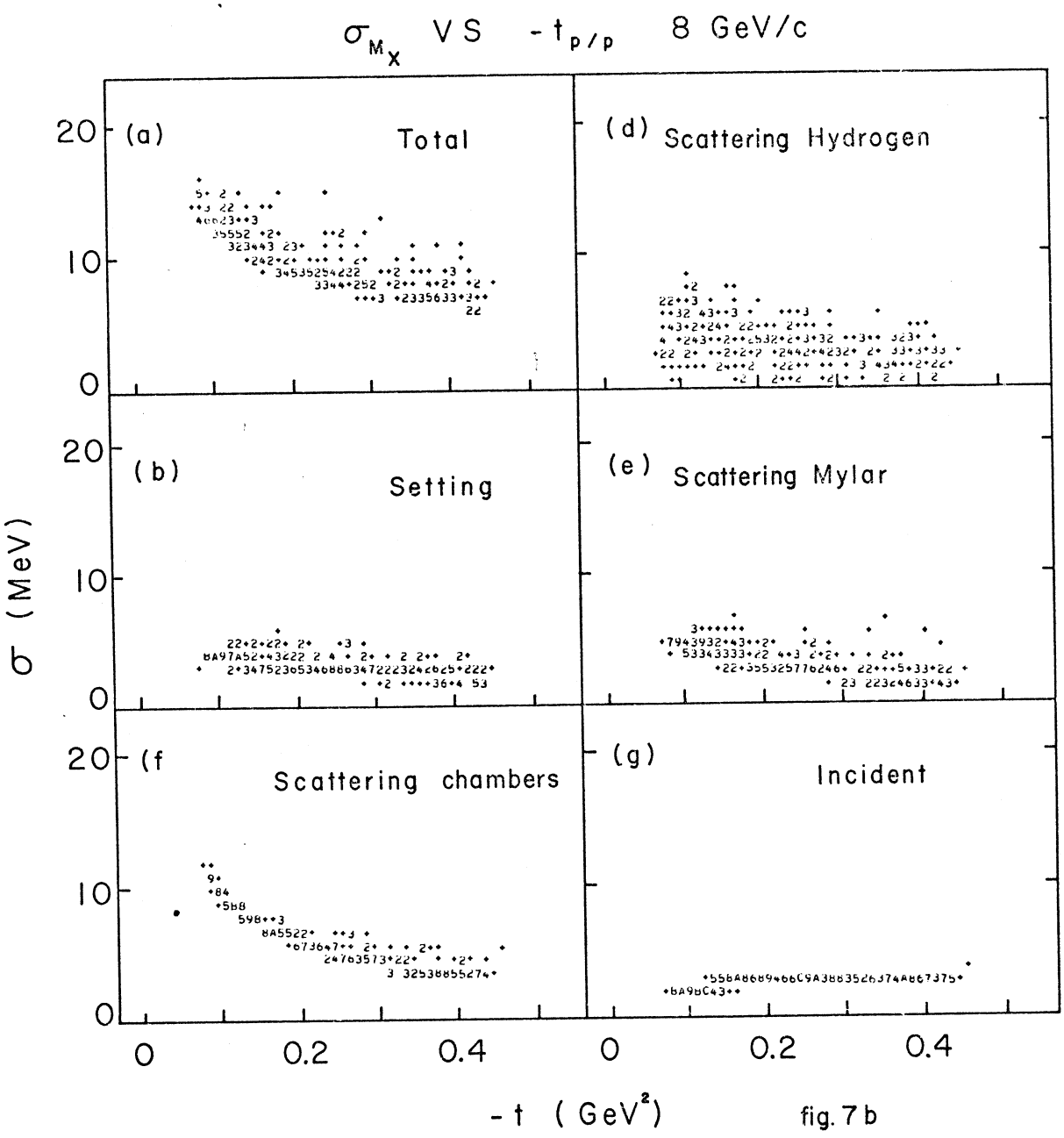
σ_{M_X} VS $-t_{p/p}$ 8 GeV/c
(a) Total
(d) Scattering Hydrogen
(b) Setting
(e) Scattering Mylar
(f) Scattering chambers
(g) Incident
σ (MeV)
$-t$ (GeV^2)
0
0.2
0.4
10
20

fig. 7b

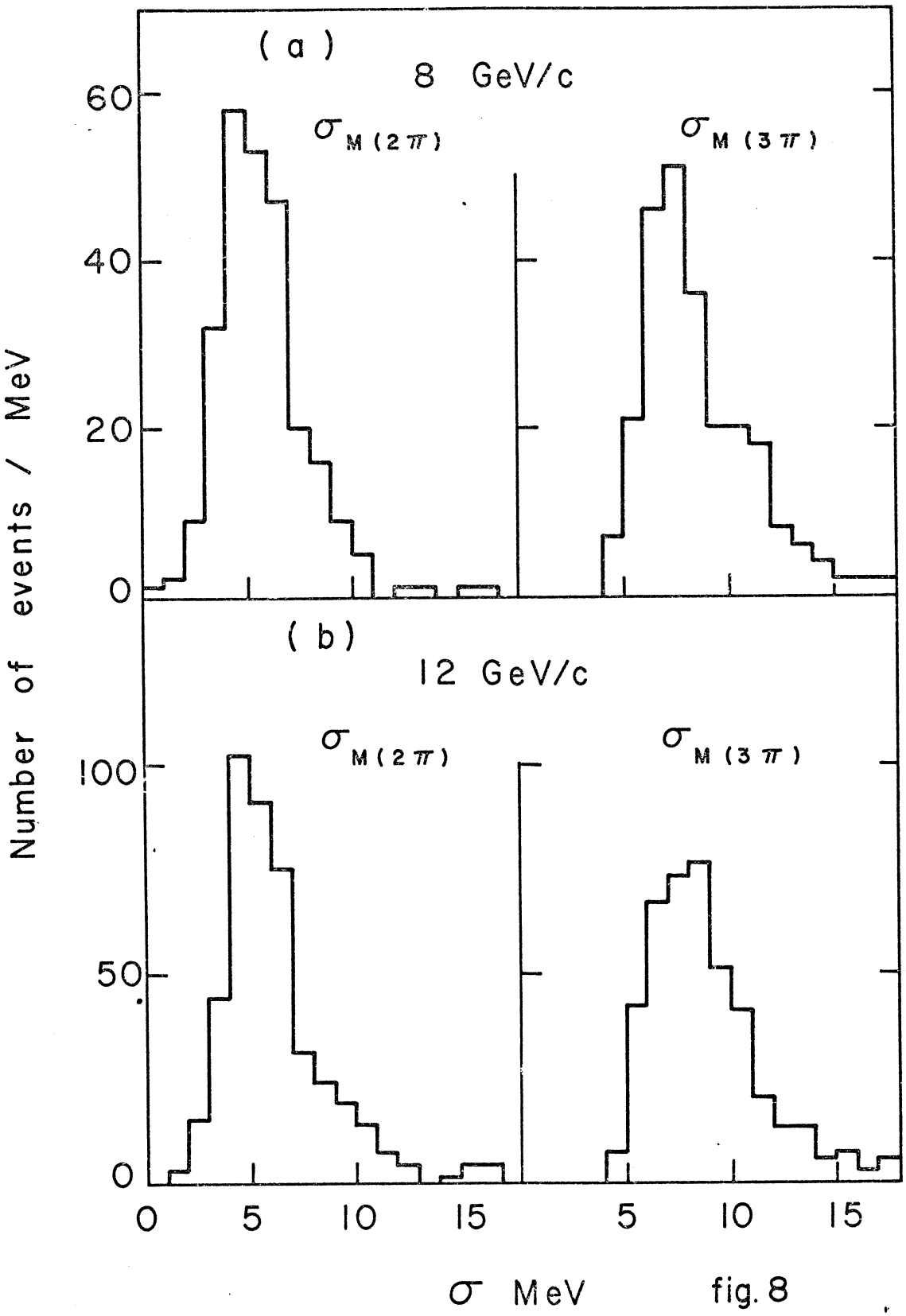
(a)
8 GeV/c
$\sigma_{M(2\pi)}$
$\sigma_{M(3\pi)}$
60
40
20
0
(b)
12 GeV/c
$\sigma_{M(2\pi)}$
$\sigma_{M(3\pi)}$
100
50
0
0
5
10
15
5
10
15
Number of events / MeV
σ MeV

fig. 8

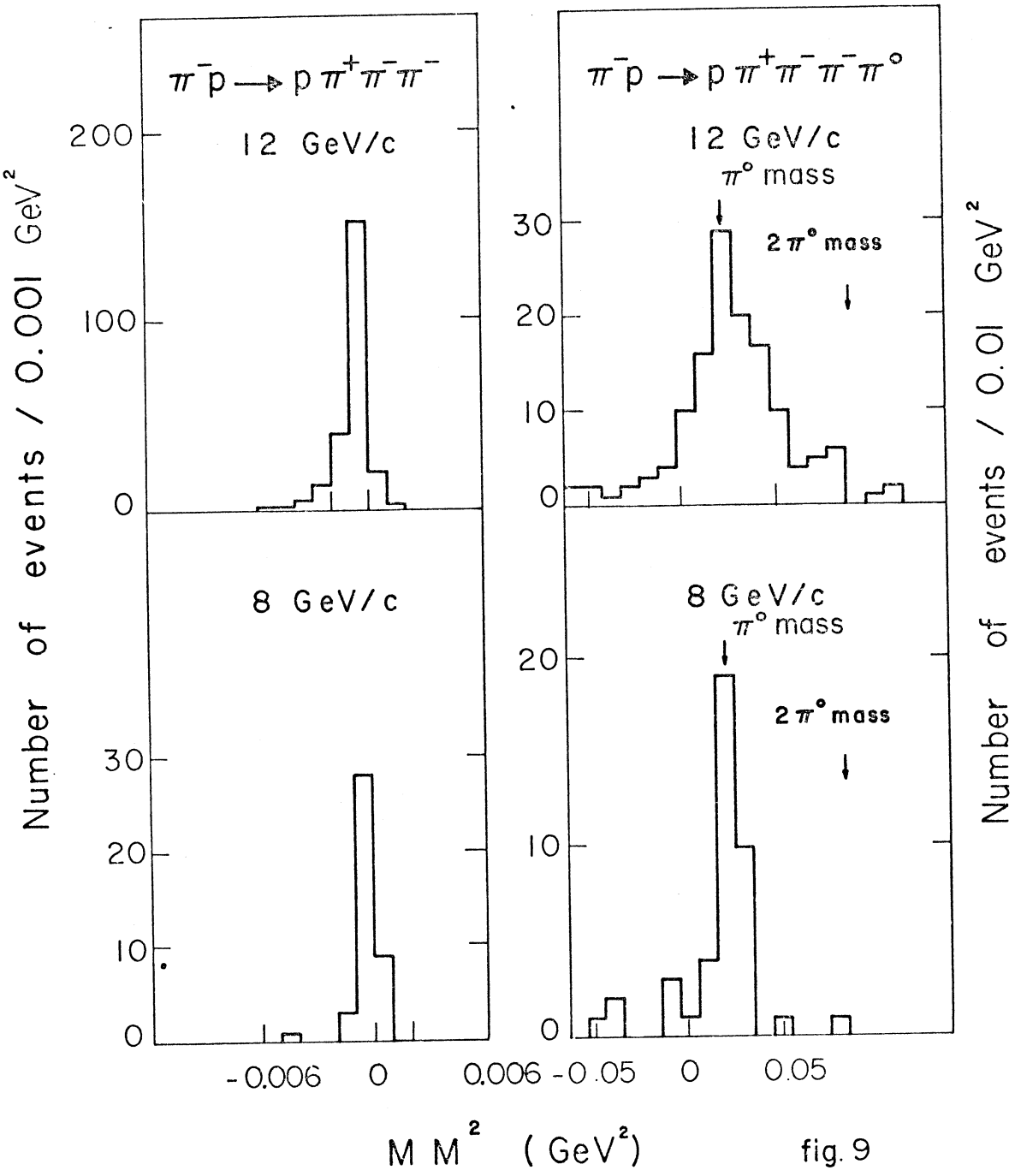
$\pi^- p \rightarrow p\,\pi^+\pi^-\pi^-$
12 GeV/c
8 GeV/c
$\pi^- p \rightarrow p\,\pi^+\pi^-\pi^-\pi^\circ$
12 GeV/c
π° mass
$2\pi^\circ$ mass
8 GeV/c
π° mass
$2\pi^\circ$ mass
Number of events / 0.001 GeV^2
Number of events / 0.01 GeV^2
200
100
0
30
20
10
0
-0.006
0
0.006
-0.05
0
0.05
M M^2 (GeV^2)

fig. 9

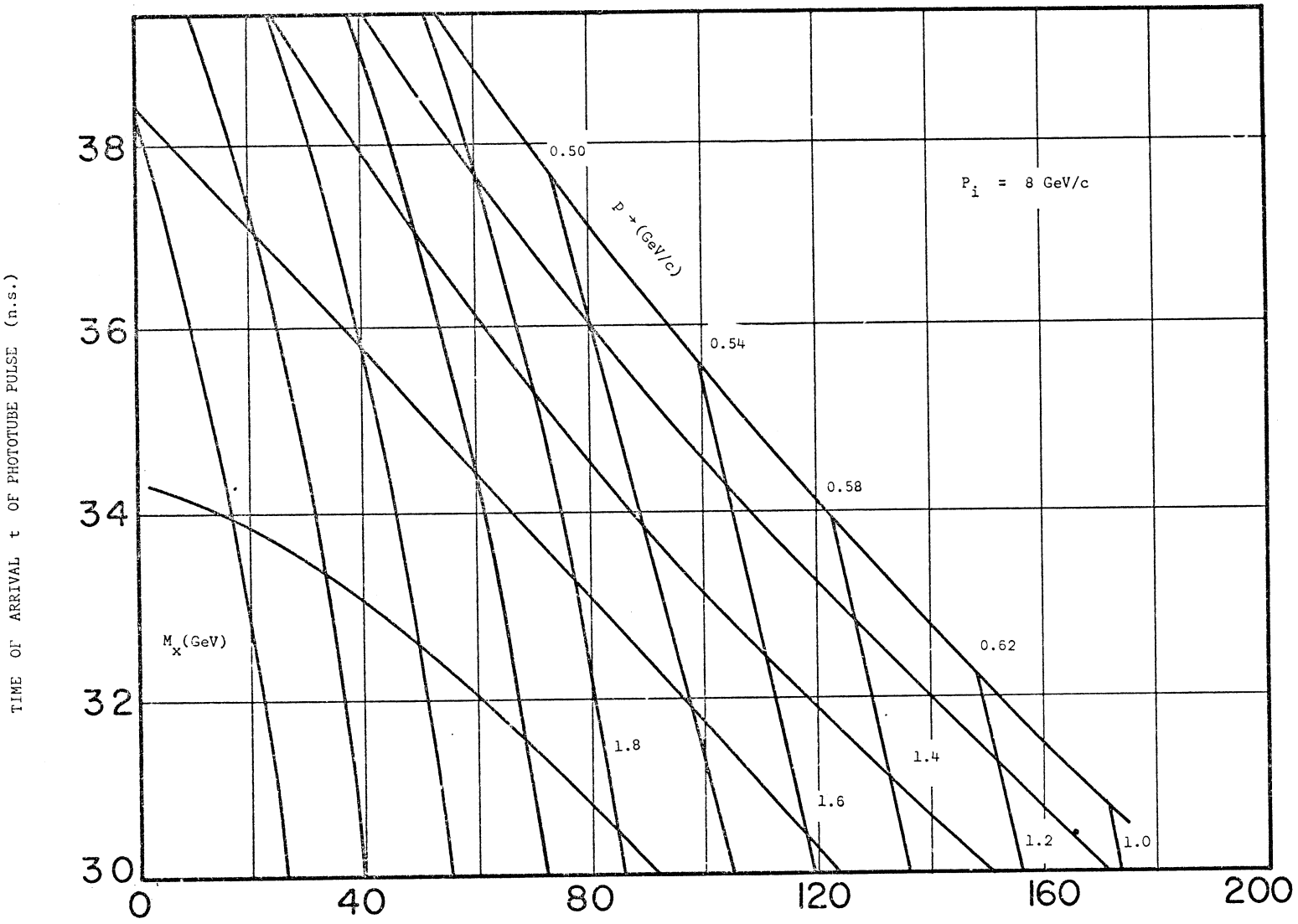

Fig. A1.1 POINT OF ARRIVAL X AT THE COUNTER (cms.)

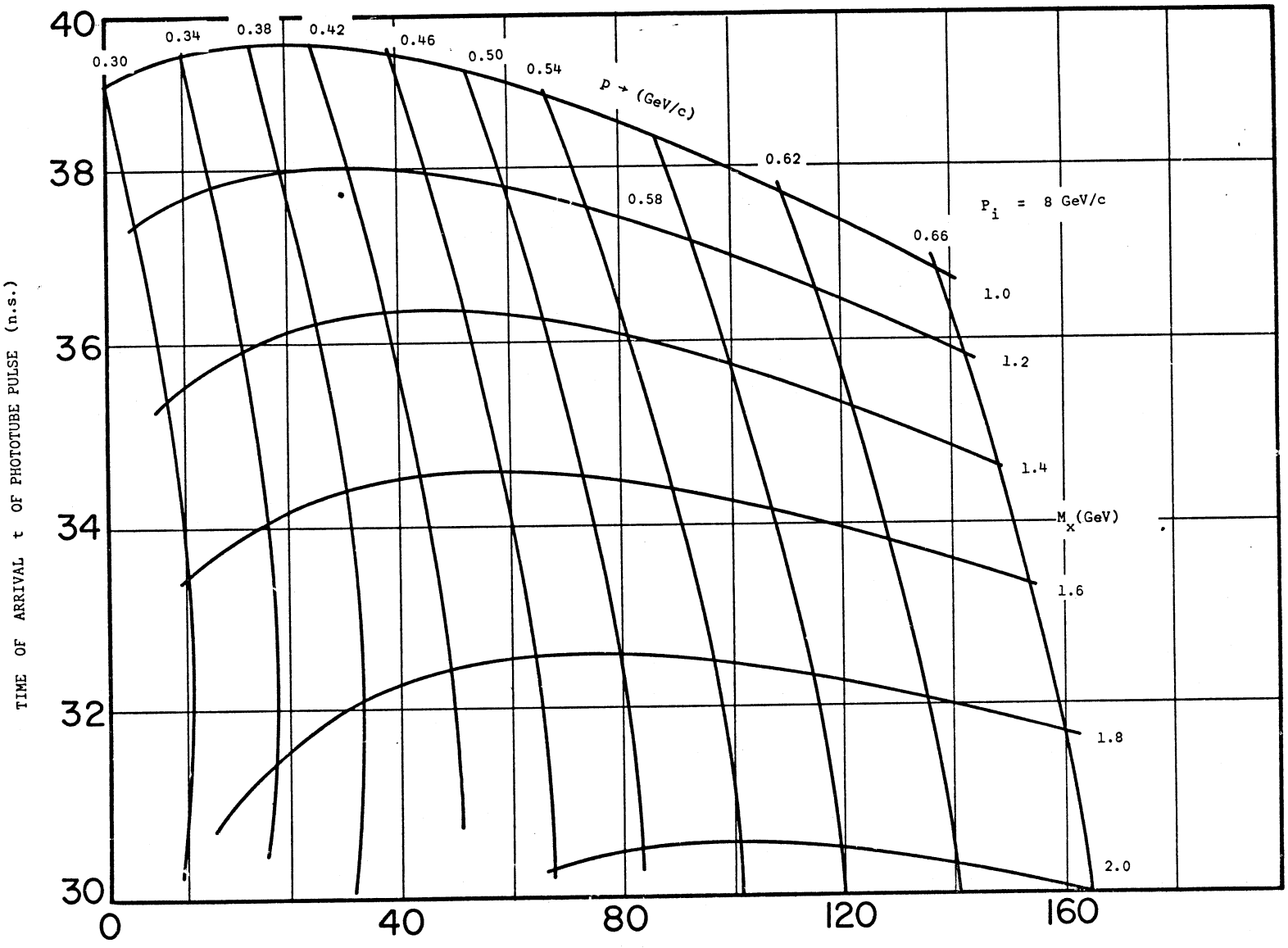

Fig. A1.2 POINT OF ARRIVAL X AT THE COUNTER (cms.)

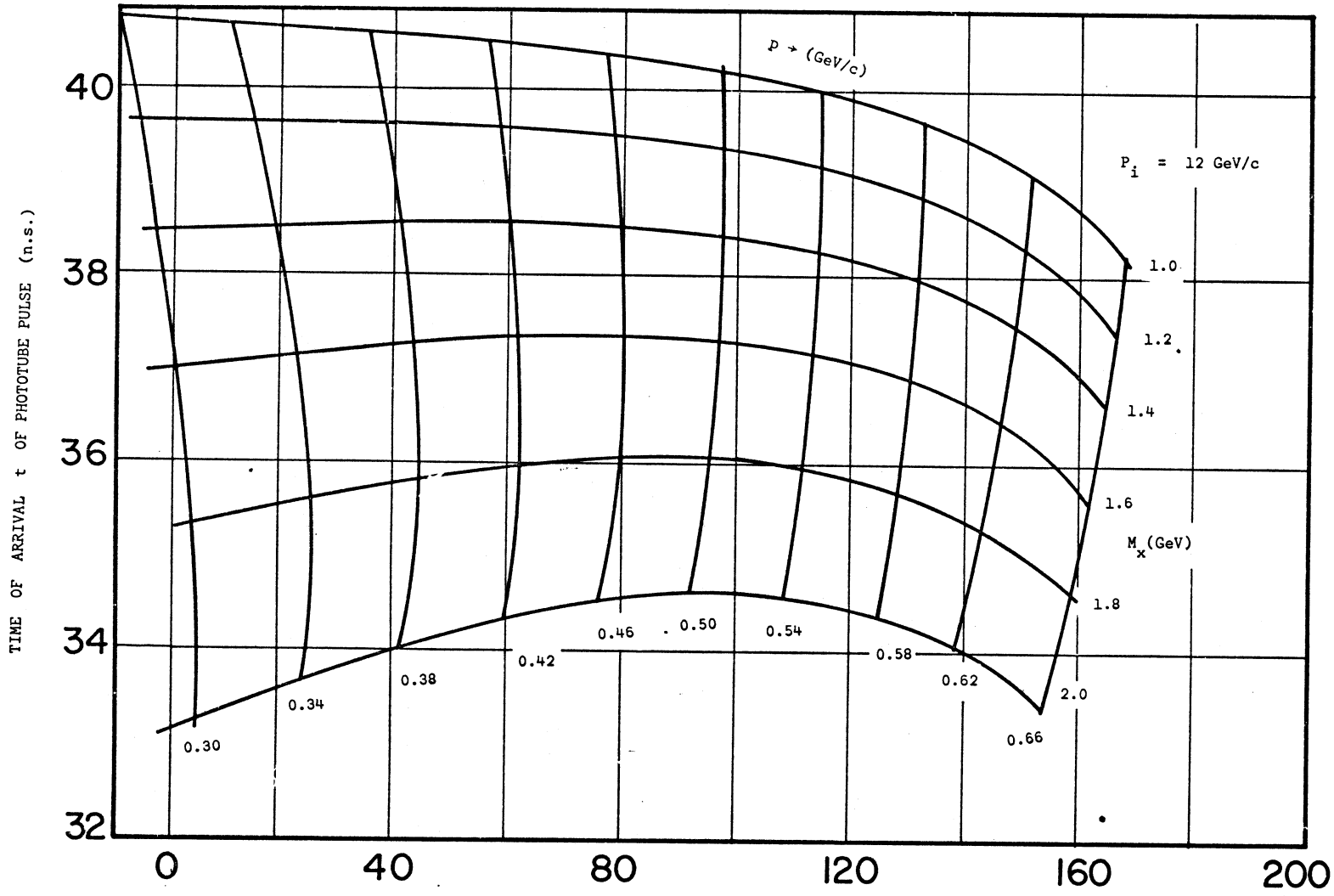

Fig. A1.3 POINT OF ARRIVAL X AT THE COUNTER (cms.)

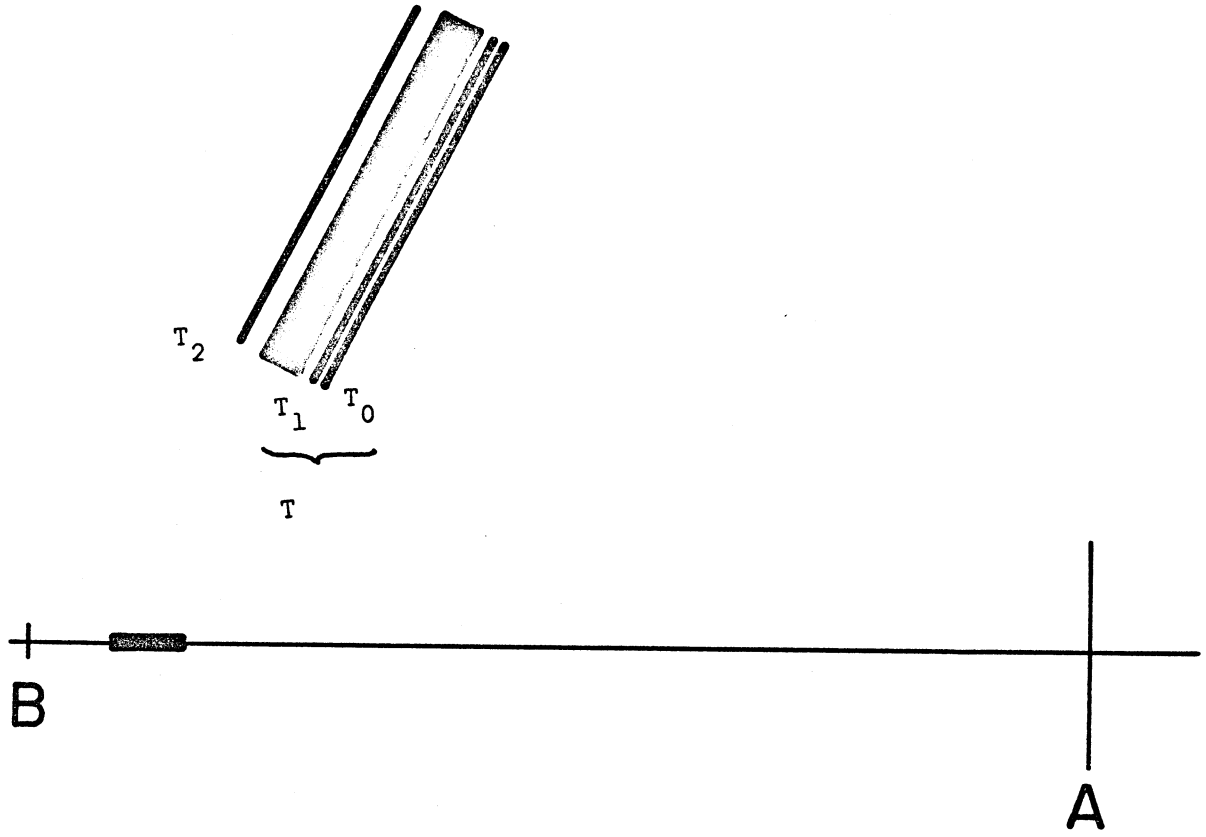

Fig. A1.4 - ARRANGEMENT OF COUNTERS